JOURNAL OF PROPULSION AND POWER
Vol. 18, No. 1, January–February 2002

Verification Tests of Carbon–Carbon Composite Grids for Microwave Discharge Ion Thruster

I. Funaki,* H. Kuninaka,† K. Toki,‡ Y. Shimizu,§ and K. Nishiyama¶
Institute of Space and Astronautical Science, Kanagawa 229-8510, Japan
and
Y. Horiuchi**
NEC Aerospace Systems, Ltd., Yokohama 224-8555, Japan

An ion beam optics for a 10-cm-diam 400-W-class microwave discharge ion thruster was fabricated and its applicability to a long-term space mission was demonstrated. The optics consists of three 1-mm-thick flat carbon–carbon composite panels with approximately 800 holes that were mechanically drilled and positioned with ± 0.02-mm accuracy. When mounted on an aluminum ring, spacing for the three grids was kept at 0.5 mm by three sets of spacers. The thruster produced an ion beam current of 140 mA with a microwave power of 32 W for plasma generation and a total acceleration voltage of 1.8 kV. Although the grid is sputtered by the impingement of slow ions produced in charge-exchange collisions between fast beam ions and neutral atoms leaking from the engine, the grid showed only slight damage even after an 18,000-h endurance test. Also, other qualification tests including a mechanical test under launch conditions as well as a thermal vacuum test simulating the spacecraft thermal environment were successfully completed. Hence, the grid system was qualified for spacecraft propulsion.

Nomenclature

d_s = screen grid diameter, m
e = elementary charge, 1.60×10^{-19}C
I_{bh} = ion beam current per hole, A
I_{eq} = equivalent current of eroded carbon, A
l_d = gap between accelerator grid and decelerator grid
l_e = effective acceleration length, m
l_g = gap between screen grid and accelerator grid
m_c = atomic weight of carbon, 12.0 g
N_0 = Avogadro number, 6.02×10^{23} mol^{-1}
n_{ph} = normalized perveance per hole, A/V$^{3/2}$
$\dot{n}$ = number of eroded carbon atoms per second, s^{-1}
t = time, s
t_s = thickness of the screen grid
V = total acceleration voltage, V
w_{ac} = weight change of accelerator grid, g/s

I. Introduction

THE Institute of Space and Astronautical Science is planning to launch a space probe in 2002 for a near-Earth asteroid exploration mission named MUSES-C, which will attempt to touchdown on the asteroid and conduct many scientific observations including returning samples from the asteroid.[1] The 500-kg MUSES-C spacecraft will be launched by a Japanese M-5 rocket and will rendezvous with an asteroid after a two-year voyage. A new technique for use of a microwave discharge ion thruster was employed[2] in which the plasmas of both the ion source and neutralizer are generated at the electron cyclotron resonance (ECR) frequency of 4.25 GHz microwave (Fig. 1). Ions created inside the ion source are extracted and accelerated by an electrostatic grid system, achieving a mission averaged specific impulse of about 3000 s. Because the spacecraft for the asteroid rendezvous mission has to provide a large delta V without gravity-assistant maneuvers, the use of a high specific impulse ion engine considerably saves propellant and, thus, increases the payload mass fraction of the spacecraft.

The use of low-thrust electric propulsion for an orbital transfer mission requires continuous engine operation for several years to achieve a required delta V. In principle, the ion engine subsystem (IES) for the MUSES-C continuously operates, excluding a touchdown sequence to the asteroid and a coasting phase. During the round trip to and from the asteroid, the IES is required to operate for more than 16,000 h. Hence, there is a concern whether the propulsion system can survive such a long-term operation. The microwave discharge has a greater lifetime capability than conventional electron bombardment-type ion sources with hollow cathodes with low work function thermionic emitters. When the hollow cathodes are excluded from the conventional ion engine's discharge chamber, the microwave engine is free from the degradation of the thermionic emitter. Also, the electrodeless feature of the microwave ion source removes internal sputtering because the ions bombard the discharge chamber wall only by its plasma potential of around 20 V (Ref. 3), and the corresponding ion bombarding energy is below the threshold of the sputtering of the chamber wall material or the screen grid (both are equipotential) as will be confirmed in the experimental results.

In addition to these features free from degradation of the discharge chamber, a quick ignition without a preheating sequence is possible just by introducing the microwave power into the thruster head. This is done by eliminating the need for a high-temperature heater, which is also considered as a life-limiting component because the heater could fail from cyclic operation. These possible life-limiting factors are of course resolved for flight model thrusters, but even after the qualification processes, a concern will remain about what is the ultimate lifetime of the engine. Furthermore, many qualification processes are still required for different cathodes. The microwave-based ion engine in principle removes these life-limiting devices, and the

Received 19 December 2000; revision received 19 June 2001; accepted for publication 19 June 2001.

*Research Associate, Space Propulsion Division, 3-1-1 Yoshinodai, Sagamihara; currently Assistant Professor, Institute of Engineering Mechanics and Systems, University of Tsukuba, Tsukuba, Ibaraki, 305-8573, Japan. Member AIAA.
†Associate Professor, Space Propulsion Division, 3-1-1 Yoshinodai, Sagamihara. Senior Member AIAA.
‡Professor, Space Propulsion Division, 3-1-1 Yoshinodai, Sagamihara. Member AIAA.
§Research Engineer, Space Propulsion Division, 3-1-1 Yoshinodai, Sagamihara. Member AIAA.
¶Research Associate, Space Propulsion Division, 3-1-1 Yoshinodai, Sagamihara. Member AIAA.
**Assistant Manager, 1st Engineering Department, 4035 Ikebe-cho, Tsuzuki.

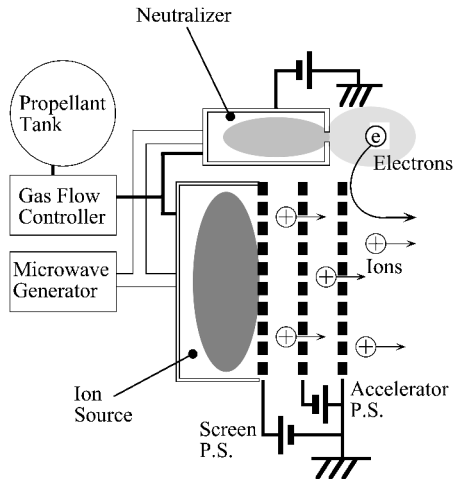

Fig. 1 Principle of microwave discharge ion thruster.

intrinsic operational ease of a microwave discharge will assure a longer lifetime and higher reliability of the microwave-driven IES. Nevertheless, sputter erosion of grid material by ion impingement will hinder the microwave engine from being totally free of degradation. Even if the ions are properly focused when they are passing through a grid hole of an accelerator grid, charge-exchange ions are produced as a result of the interaction between slow neutral atoms leaking from the screen grid and the fast ion beam. The created slow ions are attracted to the negatively biased accelerator grid and steadily erode the surface of the accelerator grid. If the erosion advances to a severe level, beyond which electron backstreaming of electrons from the neutralizer occurs due to accelerator aperture enlargement from sputter erosion, the ion extraction and acceleration in the space charge condition collapses and the thruster reaches its end of life. As for the wear of the other grids, the decelerator grid does not suffer from such wear provided the beam is focused correctly. In contrast, the screen grid also receives ion impingement from the plasma inside the discharge chamber. The described grid erosion mechanisms are considered the most critical and inevitable life-limiting factors, excluding random events that could lead to a grid-to-grid short.[4]

As a best combination of mechanical properties as well as low sputter yield, molybdenum is usually used for the ion optics. However, even molybdenum suffers from severe erosion, limiting the lifetime of the accelerator grid. One way to overcome this life-limiting issue is to employ a material with higher resistance to ion sputter damage, such as carbon. For this purpose, we employed a carbon–carbon (C/C) composite material, in which fragile graphite is reinforced with carbon fibers to survive a vibrational environment of a spacecraft launch. The C/C composite was intensively studied from the early 1990s, especially at The Boeing Company and the Jet Propulsion Laboratory as a replacement for molybdenum grids. After a successful demonstration of the first C/C ion optics,[5] C/C's lower sputter yield was confirmed.[6] However, its weak mechanical properties and difficulty in fabrication prevented its practical application, and accordingly drove researchers toward pursuing a number of fabrication techniques that improved its structural strength.[7–10] A difficulty of the C/C grid originates in its contradicted requirement: Strong mechanical properties are required in a thin plate with many holes in a large open area fraction. In spite of such difficulties, ESA and NASA continue the development of the C/C grids through contracts with commercial companies[11,12] because the C/C composite is considered as a next-generation grid material for high-performance ion engines. Until now, as far as we know, no C/C grid system was qualified for a satellite application, which demands such qualification processes as a long-term life test, and a vibrational test simulating the spacecraft launch condition.

Under these circumstances, the Institute of Space and Astronautical Science started a qualification program of a C/C grid in 1996. From our initial investigations, in contrast to the difficulty associated with large diameter C/C grids being pursued by other organizations, as far as our small 10-cm-diam engine is concerned, we believe that a flat C/C ion optics set can be precisely fabricated with enough structural strength if an appropriate fabrication technique for the C/C grid and mount system are employed. In this paper, after briefly describing the design and fabrication of engineering model (EM) grid systems, results of verification tests to check the compatibility of the grid system to the MUSES-C spacecraft are reported. These tests include a wear test to demonstrate the lifetime of the optics, a mechanical test to check the survivability of the grid system in the launch vibrational environment, a thermal vacuum test to check the compatibility to a severe thermal condition in space, and performance tests to evaluate the extracted ion beam in combination with the microwave ion source.

II. Design of the Microwave Discharge Ion Engine

A. Thruster Head of the Microwave Discharge Ion Engine

The ion thruster head is composed of a cathodeless ion source, an acceleration grid, and a neutralizer, as shown in Fig. 2. The flight model thruster has a microwave power supply for each thruster head, where power is divided into the ion source and the neutralizer. For the ion source, the microwave power, which is as much as 32 W, is transformed from a coaxial cable into a circular waveguide, and then introduced into the main discharge chamber consisting of a magnetic circuit. The ECR layer, where most of plasma generation is expected to occur, lies above the magnets, from which the ions produced diffuse to and are then extracted by the acceleration grids. Such a design not only protects the microwave antenna from sputtering by ion impingement, but also enables impedance matching of the microwave for a wide range of throttling conditions by selecting an appropriate geometry for the antenna–waveguide transformer. Accordingly, without any impedance matching device that automatically lowers the reflected microwave toward the power source, the plasma is easily ignited just after introducing the microwave into the discharge chamber, then a stable plasma is maintained both for an accelerated and for a nonaccelerated operation. In addition to plasma production, the strong magnetic field in the ion source also suppresses wall plasma losses, keeping the ions away from the chamber wall and guiding the ions toward the ion optics. For ion acceleration, the screen grid and the ion source are equipotentially biased to 1.5 kV, the accelerator grid is biased to -300 V, and the decelerator grid is grounded. Correspondingly, the microwave cable and the gas feed are insulated from the engine by an electrical insulator and a gas isolator, respectively. As for the microwave neutralizer, the microwave power is directly introduced by an antenna into a small discharge chamber which has an 18-mm inner diameter. The plasma production of the neutralizer also relies on an ECR frequency microwave discharge, and electron current is extracted and coupled to the main ion beam by biasing between the neutralizer and the thruster ground.[13] Note that no keeper electrode is needed for this system. Here the electron current is controlled to extract the same amount of electrons to neutralize the ion beam,[14] and the coupling voltage is determined to be about -30 V.

B. Grid Design

Flat, circular grids, of 10 and 12 cm diam, were fabricated from a 30-cm-square C/C panel. C/C composite is a structure consisting of fibrous carbon substrates in a carbonaceous matrix. As a carbon fiber, a pitch-based carbon fiber felt was selected, which consists of tangled continuous filaments of about 10 μm in diameter. To get additional strength and mechanical stability, the carbon matrix is deposited on the pitch-based fibers by a chemical vapor infiltration (CVI) technique.[15] This technique densifies the composite panel at temperatures beyond 1000 K and minimizes the number and the size of pores between the fibers. Resulting C/C panel properties for a breadboard model (BBM) and EMs are summarized in Table 1 (also see Ref. 16). The material strength of C/C is inferior to that of molybdenum and the state-of-the-art C/C panels. This is because the felt-type C/C does not consist of woven long carbon fibers that reinforce the C/C panel. However, the tangled microcarbon fiber

structures of the felt carbon create an isotropic composite, which can be easily machined into a desired shape with an acceptable tolerance and surface roughness. Even after the drilling, part of these microcarbon structures remains between the holes, sustaining the overall structure of the C/C plate. Hence, after the C/C composite is shaped into a thin plate, a precise mechanical drilling creates a grid hole. Fabricated grid dimensions are summarized in Table 2. A close-up view of the 3-mm-diam holes in a C/C grid is shown in Fig. 3. Note the very clean surface and that the straight hole profile without delamination, cracks, or fiber pullout is confirmed.

Other than this carbon felt, thin fiber sheets would be a good candidate for the grid fabrication. In Ref. 17, Mueller et al. fabricated a 0.46-mm-thick screen grid by piling six thin sheets consisting of pitch-based unidirectional fibers. The unidirectional tapes were compiled in different directions to obtain a quasi-isotropic C/C in a direction parallel to the surface. This panel was also reinforced by the CVI process, and larger flexural modulus compared to the felt carbon was obtained. However, the flexural modulus showed strong anisotropy that inherently depends on the direction of the unidirectional fibers, and machining becomes difficult for these plates, requiring a laser drilling that usually cannot establish a straight hole; a tapered hole is typically created.

As a result of the discussion on the grid material selection, we decided to use the felt C/C composite. In spite of adopting the CVI process and high-modulus pitch-based carbon fibers, the strength of the felt-type C/C composite grid before machining is far below that of a typical molybdenum grid, as is indicated in Table 1. The strength after the drilling will further reduce the bending modulus, and so it is possible that a problem would occur in a severe vibrational environment during spacecraft launch. To overcome this difficulty, the rigid mount system shown in Fig. 4 was designed. The C/C grid plates are mounted via ceramic spacers to an aluminum ring, and the grids are separated from each other by the spacers. Their gaps are precisely adjusted when they are torqued to the ring. With this fastened grid attachment, the grid increases its strength and the grid-to-grid gap can be controlled to ± 0.04 mm accuracy. The mechanical test result of this grid mount was good; the experimental result of vibrational test of the grid system is discussed later.

After confirming a laboratory model's successful property of the C/C grid against ion sputtering,[18,19] the mechanical design including the grid support ring shown in Fig. 4 was established in a BBM. Then we proceeded with the fabrication of EMs. Among them, the EM1 grid was used for an 18,000-h endurance test, as well as for the grid performance measurement with an EM discharge chamber.

Table 1 Material property of C/C composite sample

Property	BBM	EM1, EM2	Typical Mo (Ref. 16)
Density, g/cm^3	1.7	1.6	10.2
Tensile strength, MPa	40	87	490
Flexural strength, MPa	72	130	N/A
Tensile modulus, GPa	25	25	327
Flexural modulus, GPa	N/A	21	327
Thermal expansion, /K	2×10^{-5}	2×10^{-5}	5×10^{-5}

III. Testing of C/C Grid

A. Grid Performance with EM Thruster Head

The beam current attainable by the C/C grid was 140 mA for EM2 at a xenon flow rate of 0.23 mg/s and a microwave power of 32 W. Corresponding ion beam production cost is 229 W/A, and propellant

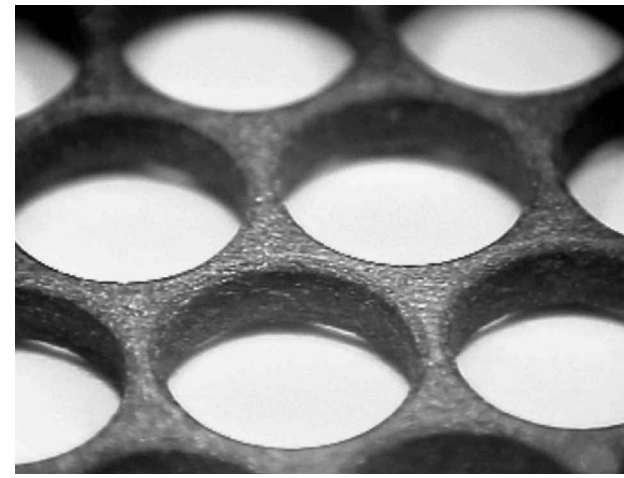

Fig. 3 Closeup view of EM1 screen grid.

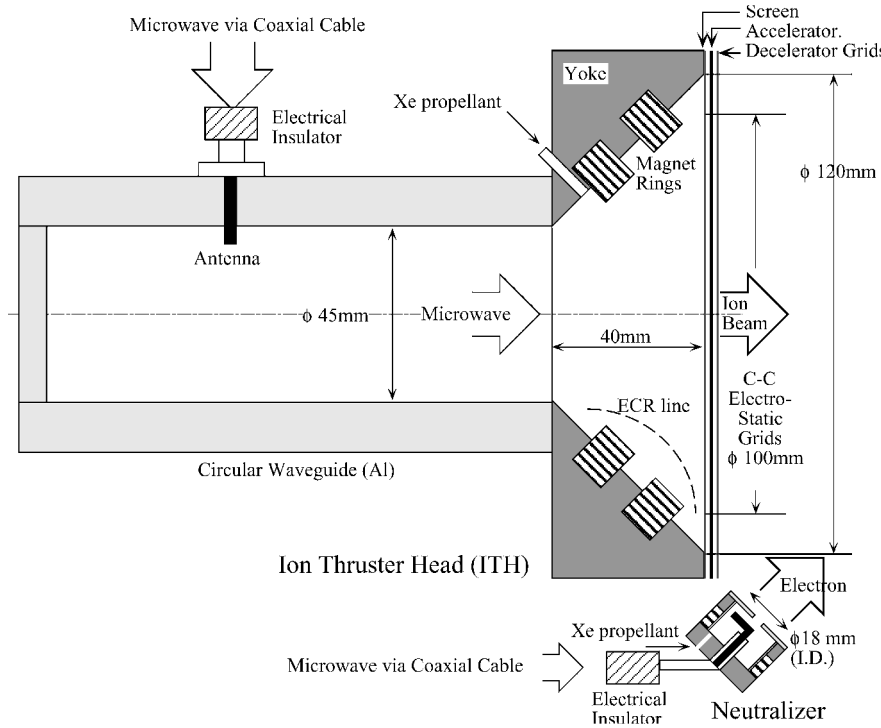

Fig. 2 Schematics of 10-cm-diam microwave discharge ion thruster head.

Table 2 Ion optics geometry

Property	BBM	EM1	EM2
Objective	Initial fabrication and preliminary test	Endurance test	Optimized performance
C/C fiber	Pitch-based felt	Pitch-based felt	Pitch-based felt
Grid shape	Circular, flat	Circular, flat	Circular, flat
Beam diameter, mm	120	100	105
Hole quantity	1066	720	850
Hole axial profile	Straight	Straight	Straight
Open area faction, %			
Screen	67	67	67
Accelerator	24	24	24
Decelerator	47	47	47
Hole diameter, mm			
Screen	3.0	3.0	3.0
Accelerator	1.8	1.8	1.8
Decelerator	2.5	2.5	2.5
Thickness, mm			
Screen	1	1	1
Accelerator	1	1	1
Decelerator	1	1	1
Gap			
Screen to Accelerator	0.5	0.5	0.35
Accelerator to Decelerator	0.5	0.5	0.5

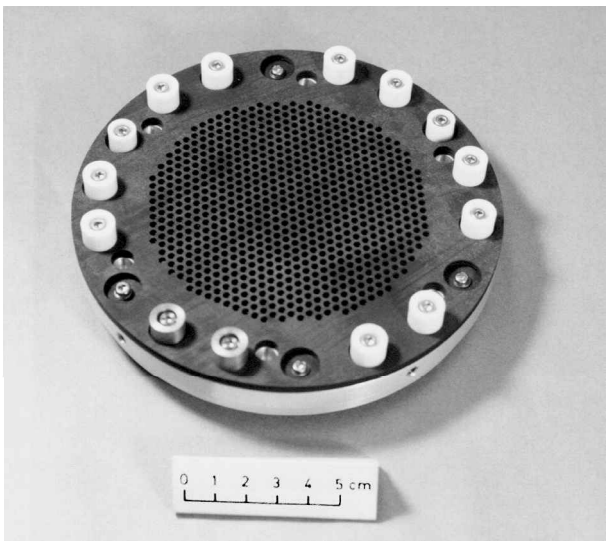

Fig. 4 Grid design; three grids mounted on a ring.

utilization efficiency is 83%. These properties are not inferior to the state-of-the-art low-power ion engine with a hollow cathode,[20] but low efficiencies of microwave power generators, which is at most 55% at this stage, make effective ion costs worse. Even so, maximum system performance for the MUSES-C exceeds 21 mN/kW, with a thrust efficiency of 50% (Ref. 21).

In spite of a thick screen grid of 1 mm in thickness, which was required to strengthen the mechanical property, the EM2 obtained a moderate value of perveance. This is checked using the normalized perveance defined as follows[22]:

$$n_{\mathrm{ph}} = \left(I_{bh} \Big/ V^{\frac{3}{2}}\right) \cdot (l_e/d_s)^2$$

We employed the effective acceleration length including the screen grid thickness presented in Ref. 23,

$$l_e = \sqrt{(l_g + t_s)^2 + d_s^2 \Big/ 4}$$

For the case of MUSES-C/EM2, $I_{bh} = 0.165$ mA, $V = 1800$ V, $d_s = 3.0$ mm, and $l_e = 2.0$ mm, resulting in $n_{\mathrm{ph}} = 0.96 \times 10^{-9}$ A/V$^{3/2}$. This is the maximum perveance for the microwave thruster head, but typical electron bombardment ion thrusters easily obtain larger values of perveance. This is mainly attributed to a low plasma density inside the microwave ion engine, in which the maximum plasma density is restricted by the cutoff density of the 4.25 GHz microwave, 2×10^{11}/cm^3, whereas for the dc discharge ion thrusters, it is easy to obtain a factor of 2–3 larger plasma density inside the discharge chamber.[24,25] One may think that the larger plasma density would be obtained by further enlarging the microwave power, but a mode hop of the discharge from the ECR to the upper hybrid resonance oppositely deteriorates ion production cost.[3] In this sense, the input microwave power should be selected to optimize the power coupling efficiency from the input microwave to the plasma. This is in contrast to the dc discharge ion engines that can easily throttle the thruster by changing the discharge parameters.[26]

Table 3 Random vibrational levels of the EM1 grid assembly

		Power spectral density (PSD)		
Axis	Grms (gravity root mean square)	Frequency, Hz	PSD Level, G^2/Hz	Slope, dB/octave
3-axis	26.8	20–100		+6
		100–1000	0.5	——
		1000–2000		−6

B. Mechanical Test

A vibrational test of the C/C grid was performed to evaluate the mechanical strength under the launch environment of the M-5 rocket. The test conditions are summarized in Table 3. Three-axis random tests were executed for the EM1 grid mounted on the aluminum ring. The resonant frequency of each grid exists around 300 Hz, but the vibrational level 10 dB higher than the fundamental level was executed from 200 to 500 Hz without damaging the grid system. At higher levels of vibration, we observed collisions between the grids, which was not prohibited even for the reinforced composite grids used in the EMs. Fortunately, no damage after the mechanical test was found, so we decided to permit the collision between the grids.

C. Thermal Vacuum Test

To demonstrate the thruster operation under a thermal environment in space, temperature measurements of the EM1 grid with the thruster head components, which consists of a discharge chamber, propellant feeding devices, and microwave/dc power supplying lines, were conducted using digital thermometers and thermocouples. In the vacuum chamber whose shroud panels were kept at

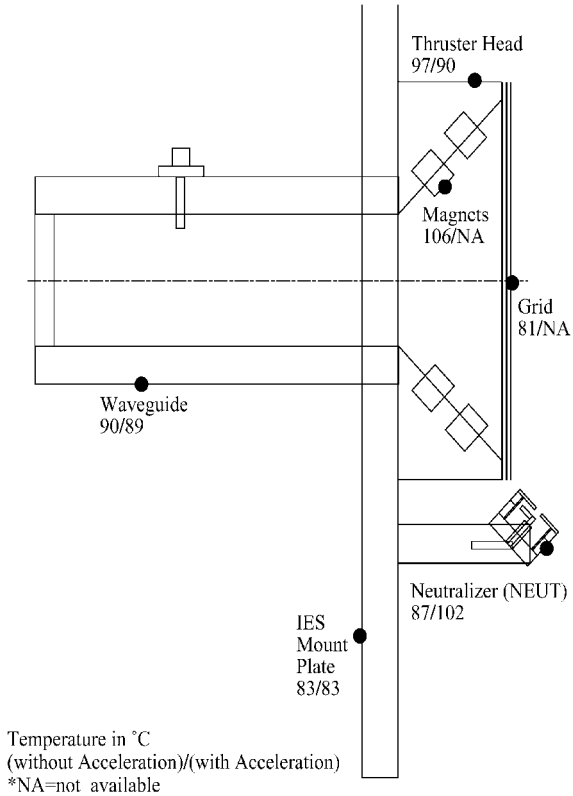

Fig. 5 Result of thermal vacuum test.

−10°C, the temperature of the IES plate, on which the thruster head is mounted, was adjusted to the nominal operational temperature of 80°C for the MUSES-C. As indicated in Fig. 5, high temperatures were observed at the surface of the magnetic circuit inside the ion source, at the grid assembly, and at the neutralizer, but they were at most 110°C. These temperatures are far below the maximum allowable temperature (200°C), which is restricted by the Sm–Co magnets. Also, no large temperature gradients were found inside the thruster head. Based on this measurement, a thermal model was created, and the thermal design for the ion engine subsystem and for the entire spacecraft was conducted.[21]

One may ask how the grid gap behaves at variable temperatures. After the grids are fastened to the mount ring in room temperature, the thruster head is heated up during engine operation to about 90°C (Fig. 5). Because the thermal expansion ratio of the C/C grid is less than that of the aluminum mount ring, if the grid system is heated up, the expanded aluminum ring will extend the carbons, resulting in a deformation of the grid system. The tensile load of the C/C composite was successfully relieved by selecting the stiffness of the supporting spacers, conserving nearly the same gap between the grids for a wide range of operational temperatures.

D. Endurance Test

For a grid wear test, the microwave ion engine was located in a 2-m-diam and 5-m-long chamber, which is evacuated by four cryogenic pumps, maintaining pressures of order 10^{-4} Pa for a xenon mass flow rate of 0.20 mg/s. Note that all pressures reported in this paper are for air, that is, indicated pressures without any correction for xenon. Conditions for the endurance test are summarized in Table 4, in which ion beam current, accelerator current, and pressure are monitored every 30 s, and others are controlled parameters. Among such parameters, the xenon mass flow rate for the ion source was adjusted to keep the ion beam current 111 ± 1 mA. As shown in Fig. 6, the EM grid assembly test started with the BBM discharge chamber in February 1997, then the discharge chamber was replaced by the EM in May 1997. The endurance test was interrupted for thrust performance measurements, a mechanical test, a thermal vacuum test, a heat cycle test, and grid performance measurements.

Table 4 Endurance test conditions for EM1 grid

Property	0–2700 h BBM ion source	2700–18,000 h EM ion source
Screen voltage, kV	1.0	1.5
Accelerator voltage, V	−300	−300
Decelerator voltage, V	0	0
Ion beam current, mA	105–120	111 ± 1
Accelerator current, mA	0.5 ± 0.05	0.5 ± 0.05
Microwave power, W		
Ion source	<35.0	32.0 ± 0.5
Neutralizer	<8.0	<8.0
Xe flow rate		
Ion source, mg/s	0.176–0.196	0.181 ± 0.006
Neutralizer, mg/s	0.028–0.058	0.049
Pressure (for air), Pa	$<6.0 \times 10^{-4}$	$<6.0 \times 10^{-4}$
Propellant utilization efficiency, %	74–84	81–86

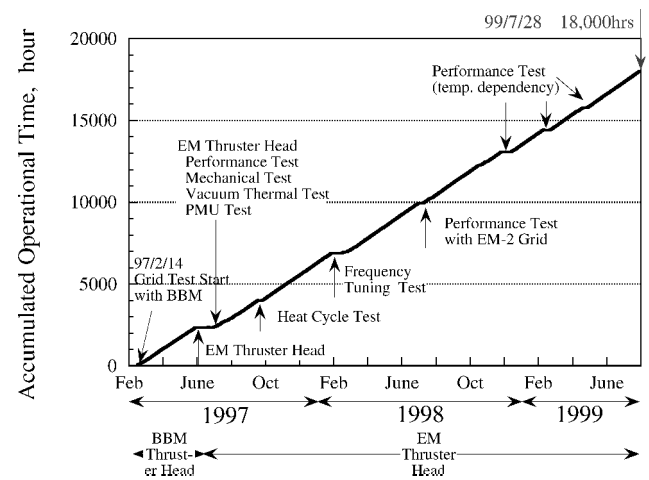

Fig. 6 Endurance test calendar.

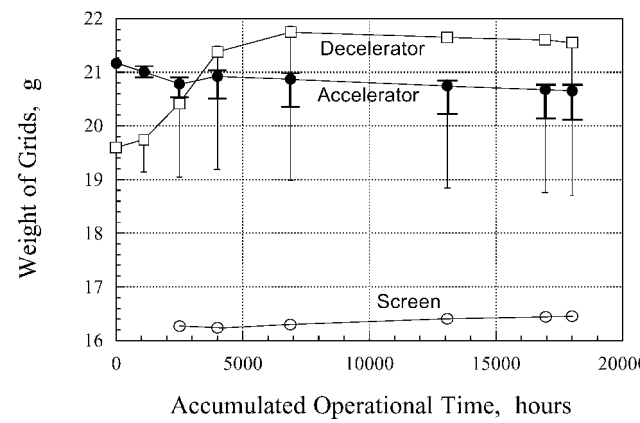

Fig. 7 Grid erosion history of the endurance test.

Other reasons for interrupting the tests include accidents related to the test facility. During the test with the EM, the observed accelerator current was 0.5 ± 0.05 mA, and the xenon mass flow rate was 0.181 ± 0.006 mg/s. These two values fluctuated both in a short period (daily) and in a long span of several months, but stayed in the cited ranges for the entire test period. Accordingly, the utilization efficiency was in a range 81–86% throughout the test.

The result of grid erosion measurement in Fig. 7 shows that the accelerator grid eroded at a rate of 28–60 μg/h. The uncertainty of the grid weight was caused by backsputtered material of titanium used for a beam dump, aluminum used for a shield suppressing electron backstreaming toward the positively biased thruster head, and molybdenum, which constitutes the neutralizer body. The deposition of these materials were monitored by quartz crystal microbalances

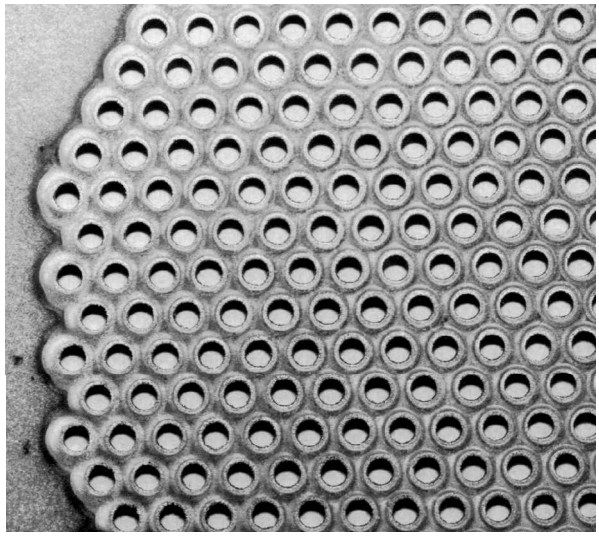

Fig. 8 Close-up view of downstream side of accelerator grid after endurance test.

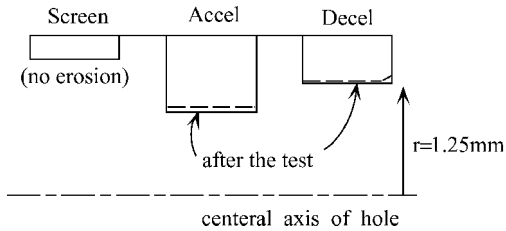

Fig. 9 Eroded grid hole profile; estimated from the image analysis.

at several chamber positions. For the first 5000 h, a large amount of both aluminum and molybdenum deposition was observed due to direct impingement of the beam ions to the shield and the neutralizer. The backsputtering amounted to 550 μg/h for the decelerator grid and 100 μg/h for the accelerator gird. After passing 5000 h, the locations of the shield and the neutralizer were changed to suppress thruster deposition. The backsputtering, hence, was reduced, and the dominant deposition was by titanium of about 8 μg/h for the decelerator grid. In addition to this weight measurement, from the micrograph analysis, the accelerator grid hole diameter was enlarged about 10% after 18,000-h operation. This accelerator grid erosion, which is also shown in Fig. 8, is acceptable, because no change of thruster performance was observed before or after the endurance test. From the weight change of the accelerator grid, averaged sputter yield of the C/C grid is calculated as follows. The sputter yield is calculated as the ratio between the equivalent current of the eroded carbon and the ion current toward the accelerator grid. The equivalent current for $w_{ac} = 28\ \mu$g/h is calculated as follows:

$$I_{eq} = \dot{n} \times e = (N_0 \times w_{ac}/m_c) \times e$$

$$= [6.02 \times 10^{23} \times (28 \times 10^{-6})/3600/(12 \times 10^{-3})]$$

$$\times 1.602 \times 10^{-19} = 6.2 \times 10^{-5}\ \text{A}$$

If the effect of backsputtered material is considered, I_{eq} could be as much as 1.3×10^{-4} A because w_{ac} could be underestimated if the plated material is not included. From these values of I_{eq}, the sputter yield for an averaged accelerator current 0.50 ± 0.05 mA is calculated as 0.11–0.28. In this prediction, the uncertainty of the accelerator current is mainly attributed to its oscillatory behavior because the measurement uncertainty is only ± 0.01 mA. Although this estimation is very simplified and without such effects as variable angles of incidence for the bombarding ions, redeposition of sputtered material, the variable of bombarding ions, etc, this low sputter yield proves the high sputter resistance of the C/C grid comparing to a Mo grid, which has a sputtering yield of 0.3 for 300 V, for example.[27] Note, however, in addition to the described endurance test, the grids were used for many performance or system integration tests and corresponding cyclic operations. Hence, the sputter yield will indicate the maximum probable yield throughout the test.

Typical grid erosion profiles after the endurance test are obtained from an image analysis, and results are summarized in Fig. 9. If one assumes that the weight loss of the accelerator grid is due solely to hole wall erosion, one would have expected a hole diameter increase of between 7 and 13%, which is similar to what was deduced through image analysis. Contrary to the accelerator grid, no erosion was observed for the screen grid. As one can see in Fig. 6, the history of the screen grid weight is available from 2700 h. The screen grid was unintentionally broken and was replaced by a backup grid at 2700 h; from that time on, no change of weight was found. This is because the microwave ion source does not require the screen grid to be biased negative relative to the discharge plasma potential as is typically done with dc-type discharge chambers. The endurance test demonstrated that the plasma potential inside the ion source is likely maintained below the threshold energy of the screen grid material, resulting in no screen grid erosion. In contrast, the decelerator grid weight increased because of titanium and other material contamination as was mentioned before. The photomicrograph of the decelerator grid (Fig. 10) also showed enlargement of the hole diameter. Unlike the accelerator grid, for which every hole is equally eroded, the eroded profile of the decelerator grid depends largely on its radial position. Enlarged downstream surface holes showed a hexagonal profile in Fig. 10, but these hexagonally eroded holes are restricted to about 10 holes near the grid center. Hence, the averaged erosion rate of the decelerator was very small, and the entire beam extraction performance did not deteriorate. This decelerator hole enlargement near the grid center is likely caused by large beam divergence, which is attributed to the case of small perveance, small l_d/d_s, and large net-to-total acceleration voltage ratio.[28] Hence the defocused fast ions directly impacted on the edge of the decelerator grid.[29] Because the grid-to-grid gap is precisely controlled by the rigid support design, nonuniform distribution of perveance is attributed to the plasma profile inside the ion source. The ion beam has an annular shape whose ion current density has a maximum at a position about 3 cm off the axis, and a minimum current density exists at the centerline where the waveguide is positioned.[30] Note that the microwave has enhanced plasma production only near the surface of the magnets (Fig. 2).

The normalized perveance per hole n_{ph} is very important in the discussion of grid erosion rate. An ion thruster with large perveance usually means a high-performance thruster with a large thrust density; however, the large perveance can cause direct ion bombardment as a result of grid hole misalignment, nonuniform grid spacing, or a radial plasma profile. Thus, not only small n_{ph} but also too large n_{ph} will induce the direct impact of ions on the decelerator grid and even the accelerator grid. In contrast, moderate n_{ph} is obtained for the microwave engine; as already described, the EM1 endurance test showed a bit smaller n_{ph} than that of typical dc discharge thrusters

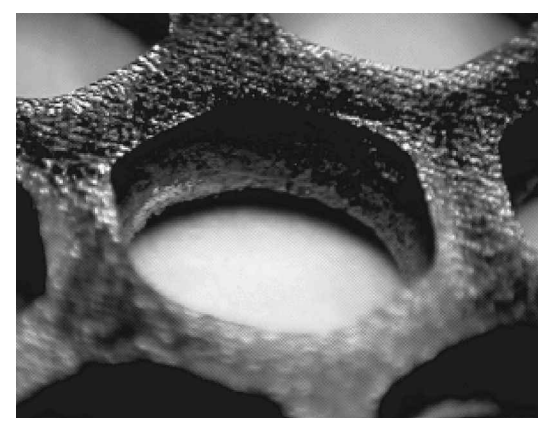

Fig. 10 Close-up view of downstream side of decelerator grid near the center after endurance test.

ranging from 1×10^{-9} to 2×10^{-9} A/V$^{3/2}$. The smaller n_{ph} also reduces the charge-exchange ions produced along the ion beam. The small n_{ph} of the microwave discharge thruster is attributed to low plasma density below the cutoff density for the input microwave. In addition to the low sputter nature of the C/C composite grid, a tuned microwave ion source optimized for this low plasma density, in this case, greatly contributes to establish longer lifetime more than 18,000 h.

As for the sputtering inside the discharge chamber, even after the endurance test, only a small amount of contamination was found inside the discharge chamber. Most of the contamination originated from the Sm–Co magnets, which are sputtered by the impingement of ions accelerated by a space potential of several tens of volts. No apparent contamination of carbon was found. Because the Sm–Co contamination amounts to only a few atomic layers on the surface of the chamber, no change of performance was confirmed. This proves that the cathodeless microwave discharge generates a clean ion source that is almost free of contaminants.

IV. Conclusions

C/C composite ion optics were developed for a microwave ion thruster being prepared for the asteroid rendezvous mission MUSES-C. Three C/C grids, which have an effective diameter of 10 cm for extracting ions, consist of a flat plate with about 800 holes, and were made from felt-type carbon matrix densified by chemical vapor infiltration processes. To supplement the weak structural properties accompanying this thin plate, the C/C grids were directly fastened to ceramic insulator spacers, and mounted on an aluminum mount ring. Thus, the grid system was confirmed to survive the vibrational environment of launch. Also, a wear test of the optics for 18,000 h proved that the low-sputter C/C material is effective in suppressing erosion. These results showed good applicability of the C/C grid system for the MUSES-C spacecraft.

Acknowledgments

The authors would like to acknowledge the valuable fabrication and support by NEC Corporation and Toyo Tanso Co., Ltd.

References

[1]Kawaguchi, J., Uesugi, T., Fugiwara, A., and Saitoh, H., "The MUSES-C, Mission Description and Its Status," Acta Astronautica, Vol. 45, No. 4–9, 1999, pp. 397–405.

[2]Toki, K., Kuninaka, H., Funaki, I., Nishiyama, K., and Shimizu, Y., "Development Status of a Microwave Ion Engine System for the MUSES-C Mission," *Proceedings of the 26th International Electric Propulsion Conference*, The Japan Society for Aeronautical and Space Sciences, Tokyo, 1999, pp. 753–760.

[3]Funaki, I., Kuninaka, H., Toki, K., and Satori, S., "Plasma Diagnostics and Numerical Modeling of a Microwave Ion Engine," AIAA Paper 98-3341, July 1998.

[4]Brophy, J. R., Polk, J. E., and Rawlin, V. K., "Ion Engine Service Life Validation by Analysis and Testing," AIAA Paper 96-2715, July 1996.

[5]Hedges, D. E., and Meserole, J. S., "Demonstration and Evaluation of Carbon–Carbon Ion Optics," *Journal of Propulsion and Power*, Vol. 10, No. 2, 1994, pp. 255–261.

[6]Meserole, J. S., "Measurement of Relative Erosion Rates of Carbon–Carbon and Molybdenum Optics," AIAA Paper 94-3119, June 1994.

[7]Meserole, J. S., Brophy, J. R., and Brown, D. K., "Performance Characteristics of 15-cm Carbon–Carbon Composite Grids," AIAA Paper 94-3118, June 1994.

[8]Mueller, J., Brown, D. K., Garner, C. E., and Brophy, J. R., "Fabrication of Carbon–Carbon Grids for Ion Optics," *Proceedings of the 23rd International Electric Propulsion Conference*, The Electric Rocket Propulsion Society, Seattle, 1993, pp. 1041–1049.

[9]Garner, G. E., and Brophy, J. R., "Fabrication and Testing of Carbon–Carbon Grids for Ion Optics," AIAA Paper 92-3149, July 1992.

[10]Kitamura, S., Hayakawa, Y., Kasai, Y., and Ozaki, T., "Fabrication of Carbon–Carbon Composite Ion Thruster Grids—Improvement of Structural Strength," *Proceedings of the 25th International Electric Propulsion Conference*, The Electric Rocket Propulsion Society, Cleveland, OH, 1997, pp. 586–593.

[11]Groh, K. H., Leiter, H. J., and Löb, H. W., "Design and Performance of the New RF-Ion Thruster RIT15," AIAA Paper 98-3344, July 1998.

[12]Patterson, M. J., Domonkos, M. T., Foster, J. E., Haag, T. W., Mantenieks, M. A., Pinero, L. R., Rawlin, V. K., Sarver-Verhey, T. R., Soulas, G. C., Sovey, J. S., and Strzempkowski, E., "Ion Propulsion Development Activities at NASA Glenn Research Center," AIAA Paper 2000-3810, 2000.

[13]Funaki, I., Satori, S., and Kuninaka, H., "Low-Power Microwave Electron Source for Ion Engine Neutralizer," *Japanese Journal of Applied Physics*, Vol. 37, Pt. 1, No. 7, 1998, pp. 4228, 4229.

[14]Kuninaka, H., Funaki, I., Shimizu, Y., and Toki, K., "Status on Endurance Test of Cathode-Less Microwave Discharge Ion Thruster," AIAA Paper 98-3647, July 1998.

[15]Buckley, J. D., "Carbon–Carbon, An Overview," *Ceramic Bulletin*, Vol. 67, No. 2, 1988, pp. 364–368.

[16]*Metal Data Book*, edited by Japan Inst. of Metals, Maruzen, Tokyo, 1984, p. 35 (in Japanese).

[17]Mueller, J., Brophy, J. R., and Brown, D. K., "Design, Fabrication and Testing of 30-cm Diam Dished Carbon–Carbon Ion Engine Grids," AIAA Paper 96-3204, 1996.

[18]Kuninaka, H., Satori, S., and Horiuchi, Y., "Continuous Operation Test of Microwave Discharge Ion Thruster System," AIAA Paper 95-3070, July 1995.

[19]Kuninaka, H., and Satori, S., "Development of Microwave Discharge Ion Thruster for Asteroid Sample Return Mission," AIAA Paper 96-2979, July 1996.

[20]Patterson, M. J., "Low-Power Ion Thruster Development Status," AIAA Paper 98-3347, July 1998.

[21]"Outline of the MUSES-C Project," Inst. of Space and Astronautical Science, Kanagawa, Japan 2000 (in Japanese).

[22]Kaufman, H. R., "Technology of Electron-Bombardment Ion Thrusters," *Advances in Electronics and Electron Physics*, Vol. 36, Academic Press, New York, 1974, pp. 265–373.

[23]Patterson, M. J., "Low-I_{sp} Derated Ion Thruster Operation," AIAA Paper 92-3203, July 1992.

[24]Okawa, Y., "Experimental Evaluation of 30 cm Ion Thruster Performance," *Proceedings of the 21st International Symposium on Space Technology and Science*, Sanbi Insatsu Co., Tokyo, 1998, pp. 1944–1949.

[25]Matossian, J. N., and Beattie, J. R., "Plasma Properties in Electron-Bombardment Ion Thrusters," AIAA Paper 87-1076, May 1987.

[26]Wilbur, P. J., Rawlin, V. K., and Beattie, J. R., "Ion Thruster Development Trends and Status in the United States," *Journal of Propulsion and Power*, Vol. 14, No. 5, 1998, pp. 708–715.

[27]Matsunami, N., Yamamura, Y., Ichikawa, Y., Itoh, N., Kazumata, Y., Miyagawa, S., Morita, K., Shimizu, R., and Tawara, H., "Atomic Data and Nuclear Data Table," Academic Press, New York, Vol. 13, No. 1, 1984.

[28]Aston, G., and Kaufmann, H. R., "Ion Beam Divergence Characteristics of Three-Grid Accelerator Systems," *AIAA Journal*, Vol. 17, No. 1, 1979, pp. 64–70.

[29]Nakano, M., and Tachibana, T., "Lifetime Model of a 3-Grid Ion Engine Grid System," *Proceedings of the 22nd International Symposium on Space Technology and Science*, Sanbi Insatsu Co., Tokyo, 2000, pp. 315–318.

[30]Ohtaki, M., "Beam Diagnostics of a Microwave Ion Engine," M.S. Thesis, Dept. of Aerospace Engineering, Nihon Univ., Tokyo, Japan, March 1997 (in Japanese).